DETAILED ANALYSIS OF MEASUREMENT RESULTS OF FLANKING TRANSMISSION ACROSS A JUNCTION COMPOSED OF DOUBLE WALLS CARRIED OUT ON A HALF SCALED TEST BENCH.

Charlotte Crispin, Christian Mertens and Arne Dijckmans

Belgian Building Research Institute, Acoustics Division, Brussels, Belgium
email: charlotte.crispin@bbri.be

This article presents an exhaustive analysis of flanking transmission across a junction composed of double walls. The analysis is mainly based on measurements carried out on a half scaled test bench where all element dimensions have been reduced by a factor 2 compared to the specifications of the standard ISO 10848. To show the same physical phenomena, the ratio between the wavelength and the wall dimensions have to be maintained. This means that the frequency range of interest has been increased by a factor 2. The test bench offers many advantages like an easy handling of elements and a significant reduction in construction costs. The measurement results are also used for the calibration of a FEM model, an SEA model and a wave based model.
Keywords: Measurement, K_{ij}, double walls, simulation

1. Introduction

Currently, the attenuation of the flanking transmission for junctions composed of double walls is closely studied by various researchers [1, 2, 3]. Indeed, although this junction is commonly found in buildings, predictive formulas don't exist yet in the EN-12354 standard. These recent articles allowed to understand and to edit representative formulas for these kind of junctions but were solely based on numerical simulations. This paper presents an analysis of experimental results obtained on a half scaled test bench. The results are discussed and are confronted to the theoretical models.

According to [4, 5], it is possible to use scaled models if the wavelengths in the structure-borne sound fields are also scaled in the same way. To ensure the same vibration behaviour in the small-scale setup and a full-scale setup (with dimensions according to the standard 10848), the ratio between the wavelength and the dimension of the elements must be maintained. This also implies that the materials must have the same longitudinal wave velocity in the two cases. Decreasing all dimensions of the walls by a factor 2 thus increases the frequency range of interest by a factor 2.

2. Test constructions and measurement procedure

2.1 The tested designs

The assessment of the vibration transmission reduction through a double walls rigid junction, named H-junction, was carried out on a junction composed of a single concrete floor and double gypsum blocks walls. The handling of the elements (walls and floor) was performed using a crane bridge. This made modifications of the junction design possible while keeping the same elements and ensured an accurate comparison of the H-junction measurement results with the other designs named Pi, λ, X and T-junctions (figure 1).

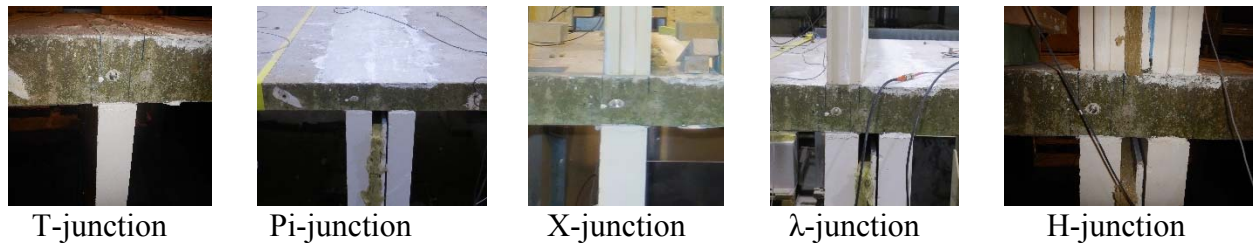| T-junction | Pi-junction | X-junction | λ-junction | H-junction |

Figure 1: Pictures of the 5 different tested designs

2.2 Setup

The H-junction was composed of a reinforced concrete floor F1-F2 (100 mm) and 4 walls (Pl1, Pl2, Pl3, Pl4) composed of gypsum blocks (70 mm). Two supporting concrete block walls (low walls) ensured the construction stability (Figure 2).
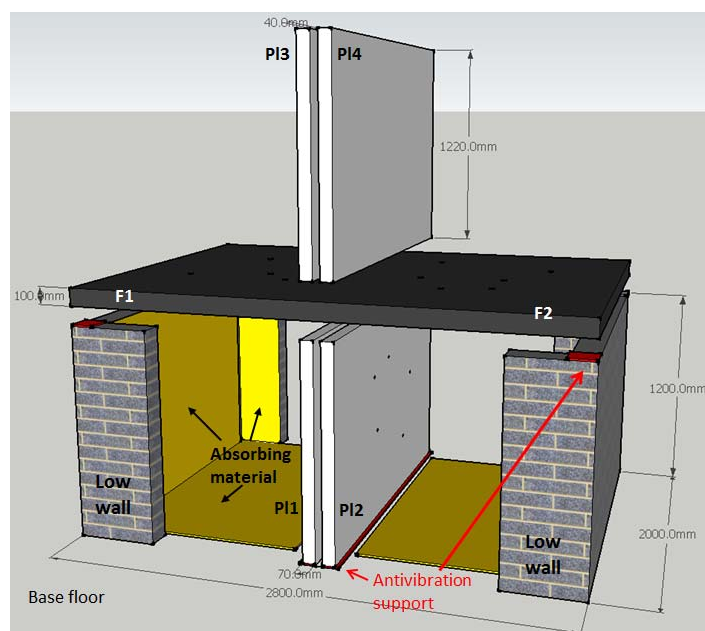

Figure 2: Illustration of the half scaled test bench

Some precautions were put in place to ensure relevant measurements as:
- Presence of absorbing material in the two cavities below the floor F1-F2.

An absorbing material was applied on the inner surfaces of the low walls, below floors F1 and F2 and on the base floor in order to minimise the airborne sound pressure generated by the hammer hits in these two cavities. In spite of it, the contribution of the airborne sound pressure on the vibration measurements was measured and subtracted from the vibration transmission measurements.
- Antivibration supports below Pl1 and Pl2 walls.

These antivibration supports were useful to avoid disturbing vibrations from the environment and to avoid the vibration transmission between wall Pl1 and wall Pl2 through the base floor. Antivibration supports were also placed between the floor F1-F2 and the low walls.
- A mortar joint between the walls and the floor.

A mortar joint was applied along the entire length between the walls (Pl1, Pl2, Pl3, and Pl4) and the floor F1-F2 to ensure a rigid coupling.
- An infilling of the cavity of the double walls.

The space between the double walls measured 40 mm. These air cavities were filled with the following 3 layers: mineral wool (20 mm), a plasterboard (12.5 mm), and a Polyethylene foam (5

mm). These infillings aimed to reduce the airborne sound transmission between Pl1 and Pl2 and between Pl3 and Pl4 through the cavities generated by the hammer hits.

- The same accelerometers positions at each design

For each design (Pi, λ, H, X and T-junction), the acceleration levels were measured at the same points in one-third octave bands.

- Verification of the basic assumptions of SEA

The main assumptions were checked such as the weak coupling between the elements, the diffuse vibration fields in each element and adequate modal overlap factors.

2.3   Test element properties

The floor F1-F2 was composed of reinforced concrete and the walls (Pl1, Pl2, Pl3 and Pl4) were composed of gypsum blocks with the following properties:

Table 1: properties of the materials

Material	Thickness [mm]	Density* [kg/m³]	Surface mass [kg/m²]	c_L** [m/s]	fc [Hz]	Edyn [N/m²]	n*** [1/Hz]
reinforced concrete	100	2300	230	3400	190	2.60E+10	0.03
gypsum blocks	70	929	65	1139	815	1.16E+09	0.05

*A boom scale was used to measure the weight of the elements and thus the density.

**The longitudinal wavespeed, c_L, was determined from the measured time of flight of a longitudinal wave generated by a hammer hit at a free edge.

***The modal density, n, was calculated by the theoretical formula $n=\pi Sf_c/c_0^2$ (with S, the surface area of the element and f_c the critical frequency of the element) and confirmed by the measurement of the driving-point mobility.

2.4   Measurement procedure

The K_{ij} measurement procedure as described in the standard ISO 10848 [6, 7] was used, with the exception that the dimensions of the elements were reduced by a factor 2 and the frequency range of interest extended from 250 Hz to 10000 Hz.

To generate a vibration field, multiple manual hammer hits with approximately the same strength were given over an area of 0.04 m² over a time period of 30 s.

Three acquisition systems with a total of 23 inputs were used. This means that the acceleration levels could be measured at 23 measurement points simultaneously (5 on F1, 5 on F2, 5 on Pl1, 5 on Pl2 and 3 on Pl3).

The structural reverberation time of each element was determined from the decay curve of the measured acceleration level with the backwards integration technique. The excitation of the element was done by an impact hammer. The final structural reverberation time of the element was determined by arithmetic averaging of 8 individual reverberation times.

3.   Measurement results

The results of the K_{ij} measurements are presented below for some transmission paths in one third-octave bands. Above 630 Hz and for the Pi, T and X designs, the weak coupling assumption between F1 and F2 is not valid but it is partially met for the λ and H designs. Therefore, the floor F1-F2 was considered as one subsystem within the meaning of SEA for all designs and the velocity level measurements for the K_{ij} involving the floor was made on the whole surface F1-F2. For information, the K_{ij} values predicted according to the standard 12354-1 [8] are given for the X-rigid junction and for the T-rigid ($K_{ij,12354,X}$ and $K_{ij,12354,T}$). The results can also be compared to the prediction formulas proposed in the article of C. Hopkins *et al.* [9] ($K_{ij,Hopkins,mid,X}$ and $K_{ij, Hopkins,mid,T}$).
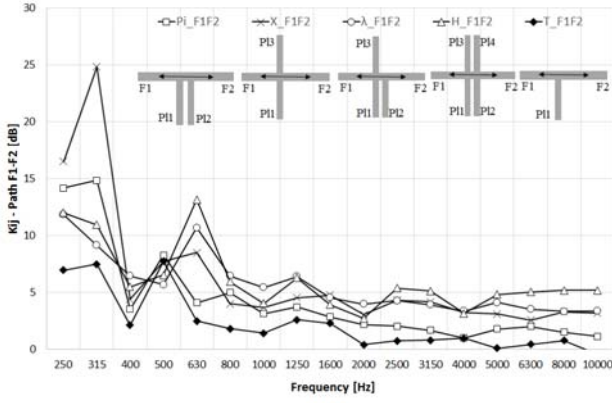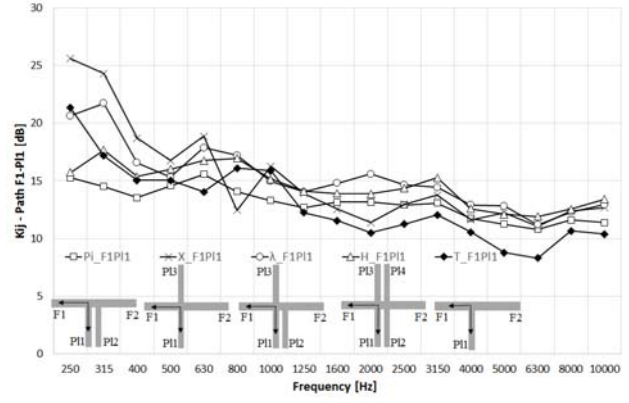
Useful information for the prediction formulas

$$\frac{m'_{L,F1}}{m'_{F1}} = 0.28 \Rightarrow K_{ij,12354,X}=1.03 \text{ dB}, K_{ij,12354,T}=-0.32 \text{ dB}$$

$$\frac{\psi}{\chi} = 0.032 \Rightarrow K_{ij,Hopkins,mid,X}=-1.69 \text{ dB}, K_{ij,Hopkins,mid,T}=-1.72 \text{ dB}$$

Figure 3: Measured K_{ij} spectra
for the transmission path F1-F2
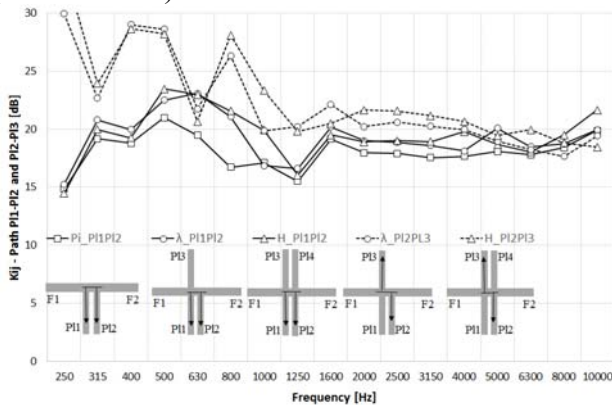

Useful information for the prediction formulas

$$\frac{m'_{L,Pl1}}{m'_{Pl1}} = 3.5 \Rightarrow K_{ij,12354,X}=10.4 \text{ dB}, K_{ij,12354,T}=7.42 \text{ dB}$$

$$\frac{\psi}{\chi} = 31.5 \Rightarrow K_{ij,Hopkins,mid,X}=18.4 \text{ dB}, K_{ij,Hopkins,mid,T}=14.6 \text{ dB}$$

Figure 4: Measured K_{ij} spectra
for the transmission path F1-Pl1

Figure 3 presents the results for the path F1-F2. The results at low frequencies (below 800 Hz) are dominated by the modal behaviour. Above 800 Hz, the K_{ij} is relatively constant with frequency for the λ and H designs but slightly decreases with frequency for the other designs. In each case, a light improvement (± 1.4 dB) of the K_{ij} is observed when a wall is added. The predicted values are lower than the measured results. However, the Hopkins prediction is calculated according to a formula which is only valid for $0{,}064 \leq \frac{\psi}{\chi} \leq 242$.

For the transmission path F1-Pl1 (Figure 4), a significant increase of the K_{ij} can be seen compared to the path F1-F2. The results show a decrease with frequency. Above 800 Hz, the difference between the different designs (T, X, Pi, λ and H) is small but relevant. For example, the K_{ij} of the H-junction is higher than that of the X-junction. This increase was expected [1]. The results for the Pi- and X-junction are similar. This confirms that for this mass ratio, the K_{ij} values for the X-junction can be used to approximate the K_{ij} for the Pi-junction as also announced by [3]. For this case, the 12354 predictions underestimate the results and the Hopkins predictions slightly overestimate them. This may be explained by the non-inclusion of an offset in the numerical simulations of Hopkins *et al.* [9] (see section 4).
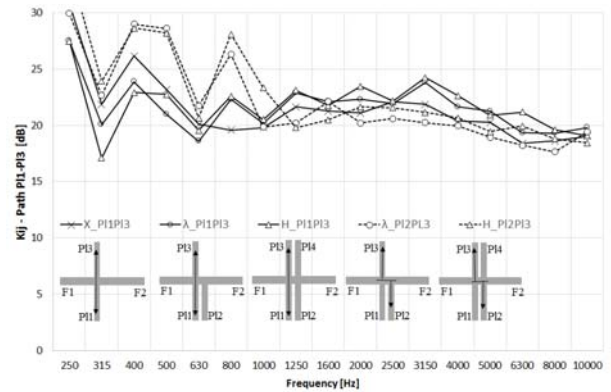

Useful information for the prediction formulas

$$\frac{m'_{L,Pl1}}{m'_{Pl1}} = 3.5 \Rightarrow K_{ij,12354,X}=19.8 \text{ dB}$$

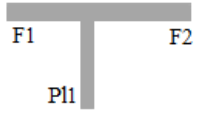$$\frac{\psi}{\chi} = 31.5 \Rightarrow K_{ij,Hopkins,mid,X}=27.9 \text{ dB}$$

Figure 5: Measured K_{ij} spectra
for the transmission path Pl1-Pl2

Useful information for the prediction formulas

$$\frac{m'_{L,Pl1}}{m'_{Pl1}} = 3.5 \Rightarrow K_{ij,12354,X}=19.8 \text{ dB}$$

$$\frac{\psi}{\chi} = 31.5 \Rightarrow K_{ij,Hopkins,mid,X}=27.9 \text{ dB}$$
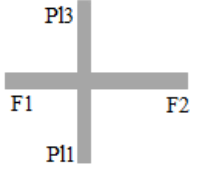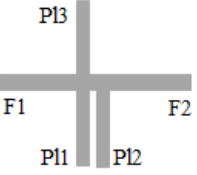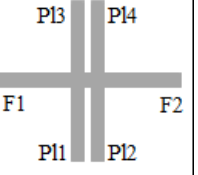
Figure 6: Measured K_{ij} spectra
for the transmission path Pl1-Pl3

In figure 5, the difference of the modal behaviour between wall Pl3 and wall Pl1 is clearly visible below 800 Hz. Above this frequency, the K_{ij} is quite constant with frequency. The transmission path Pl1-Pl2 gives lower K_{ij} values than the transmission path Pl2-Pl3, but these values converge gradually at high frequencies. This may be caused by the disturbance of the airborne noise between Pl1 and Pl2, despite the efforts to reduce this. The 12354 prediction gives a better agreement with the measurement results than the Hopkins' prediction.

For the path Pl1-Pl3 (figure 6) and above 800 Hz, the K_{ij} is quite constant over frequency even though a slightly decrease seems to begin at 3150 Hz. Surprisingly the path Pl2-Pl3 gives lower values than the path Pl1-Pl3 above 1000 Hz. For the path Pl1-Pl3, the H-junction gives a K_{ij} 1.3 dB higher than the X-junction. This is a small difference but it is relevant. Again, the Hopkins' prediction overestimates the K_{ij}.

Table 2 gives a summary of the results. The single values given in this table are an arithmetic average between 1000 Hz and 10000 Hz. For all paths, an increase of the K_{ij} (± 1dB) is observed for each added wall. This is a small but relevant difference. As expected, the non-interrupted path F1-F2 gives the lowest K_{ij} for all designs (between 0.9 and 4.6 dB) and the paths involving two light gypsum walls interrupted by the floor give the highest values (between 17.9 and 21.7 dB depending on the design). Despite efforts to reduce the disturbance of the airborne noise between Pl1 and Pl2, the measurement may underestimate the K_{ij}. Therefore, it is reasonable to conclude that the K_{ij} for the transmission path Pl1-Pl2 of the Pi-junction can be approximated by the K_{ij} of the transmission path Pl1-Pl3 of the X-junction. For the H- and λ-junction, the K_{ij} for the transmission path Pl1-Pl3 is unexpectedly higher (+1.2 dB) than for the transmission path Pl2-Pl3. For each design concerned, the path F1-Pl1 gives more or less similar results than the path F1-Pl2 because the floor F1-F2 was considered as a single subsystem.

Table 2: Summary of the measured K_{ij} single values (arithmetic mean between 1000 and 10000Hz).

	T-junction	Pi-junction	X-junction	H-junction	λ-junction
F1F2	0.9	2.1	3.6	4.2	4.6
F1Pl1	11.1	12.3	12.8	13.7	13.6
F1Pl2		12.3		13.9	14.3
Pl1Pl2		17.9		18.7	19.1
F1Pl3			14.2	13.9	14.4
F2Pl1	11.3	12.5	12.9	15.2	15.1
Pl1Pl3			20.4	21.3	21.7
F2Pl2		11.7		12.6	13.1
Pl2Pl3				19.8	20.5
F2Pl3			14.4	14.8	15.3

4. Calibration of numerical models

Before numerical models can be used with confidence, they must be validated in one way or another. Typically, this is done by a comparison with measurement results [10, 11, 12]. The results obtained on the half scaled test bench were used for the validation of three theoretical models based on FEM, SEA and the Wave Based Method (WBM). All models assume homogeneous, acoustically thin plates and unpinned junction lines. The material properties used in the simulations are given in table 1. The frequency-dependent loss factors, derived from the structural reverberation time measurements, are used as input for the internal loss factors of the plates. The results in this paper assume

a distance between the junction lines of the double walls of 4 cm, but it has been verified that a change to 11 cm has a limited influence on the simulation results.

The software used for the finite element calculation (FEM) was Actran 15. Thin shell elements were chosen for these calculations. The excitation of bending waves on the source plate was applied using three non-correlated point forces. The spatial-average velocity level was calculated on a surface which took into account the ISO 10848 requirements.

The SEA model for the double wall junctions is described in [2]. Each plate is represented by three subsystems to incorporate bending, quasi-longitudinal, and in-plane transverse waves. The coupling loss factors are determined from wave theory for semi-infinite plates under the assumption of diffuse vibration fields. While the floors F1-F2 are considered as one subsystem in the measurement, they are modelled as two subsystems in the SEA model.

Like the FEM model, the WBM model [3] takes into account the finite dimensions of the plates and includes both in-plane and bending wave vibration. The main difference with the FEM are the plate boundary conditions: while the FEM model incorporates the actual free plate boundary conditions, the WBM assumes simply supported plates. The K_{ij}-values are determined from averaged velocity level differences over five random source positions on each plate. The velocity level was analytically averaged over the entire surface of the plates.

The continuity conditions for the displacements, forces and bending moments in each junction must be evaluated at the edge of the plates. Therefore, an offset has to be introduced for the gypsum block walls (figure 7). The effect of this offset adds a supplementary displacement component and a supplementary contribution to the bending moment acting at the junction [13]. The influence of this offset is illustrated in figures 8, 9 and 10 for the three models. The non-inclusion of the offset leads to an overestimation of the K_{ij}, especially at higher frequencies.
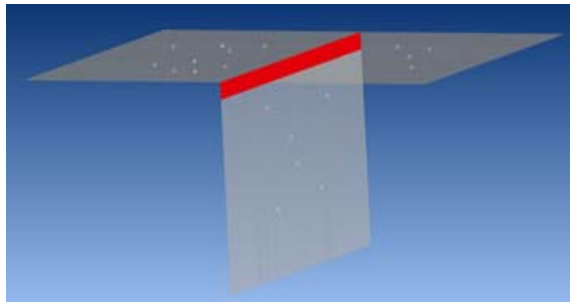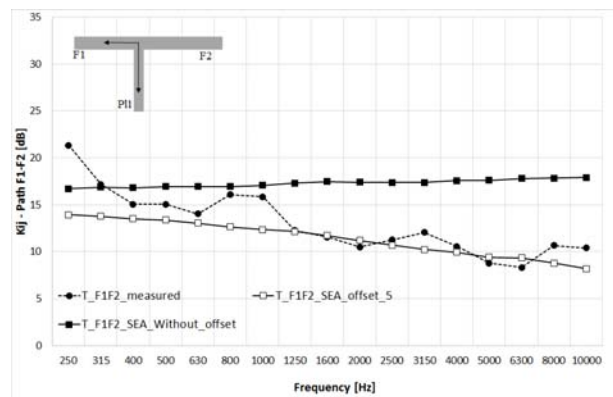

Figure 7: Illustration of the offset in the FEM model

Figure 8: SEA calculations with and without offset (5 cm) versus the measurement for the path F1-Pl1 of the T-junction.
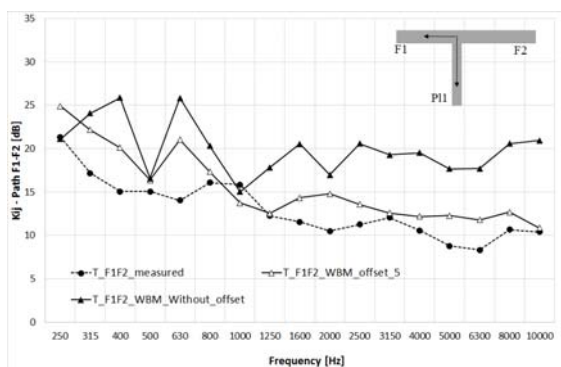

Figure 9: WBM calculations with and without offset (5 cm) versus the measurement for the path F1-Pl1 of the T-junction.
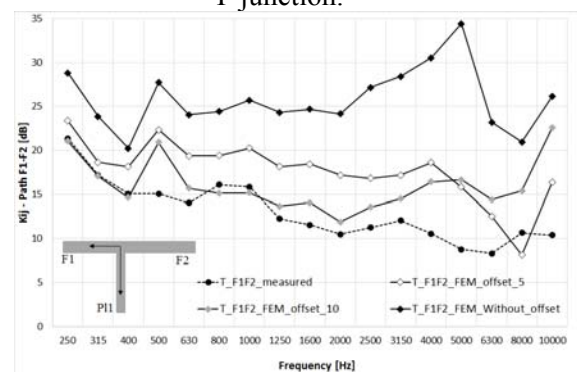

Figure 10: FEM calculations with and without offset (5 cm and 10 cm) versus the measurement for the path F1-Pl1 of the T-junction.

The figures 11 to 15 present a comparison of the numerical simulations per transmission path for the H-junction. For the SEA and WBM an offset of 5 cm was taken into account and for the FEM, the offset was 10 cm.
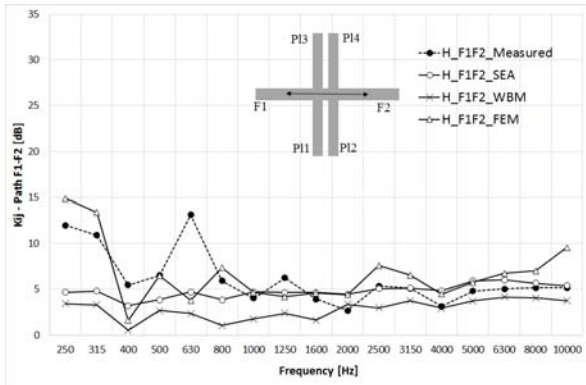

Figure 11: The SEA, WBM, FEM calculations with offset versus the measurement for the path F1-F2 of the H-junction.
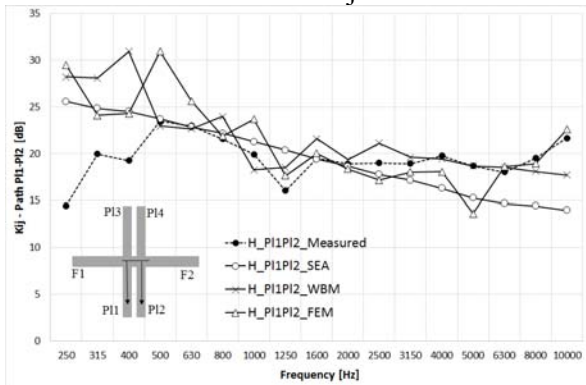

Figure 12: The SEA, WBM, FEM calculations with offset versus the measurement for the path F1-Pl2 of the H-junction.

Figure 13: The SEA, WBM, FEM calculations with offset versus the measurement for the path Pl1-Pl2 of the H-junction.
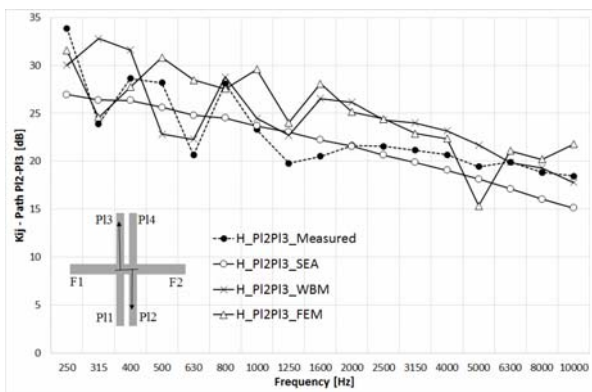

Figure 14: The SEA, WBM, FEM calculations with offset versus the measurement for the path Pl1-Pl3 of the H-junction.

Figure 15: The SEA, WBM, FEM calculations with offset versus the measurement for the path Pl2-Pl3 of the H-junction.
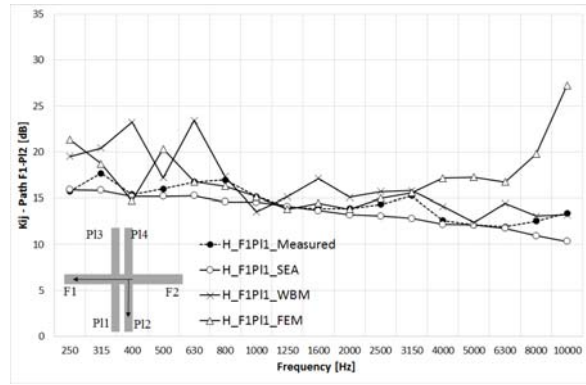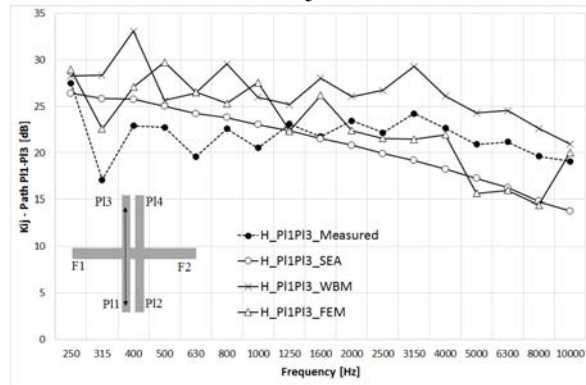
A first analysis shows that the three numerical methods are equally valid. On the ensemble of these simulations, the WBM shows a mean difference of 3 dB compared to the measured values and a maximum difference of 14 dB. The SEA shows a mean difference of 2 dB and a maximum difference of 11 dB and FEM gives a mean difference of 3 dB with a maximum of 16 dB (at 10000 Hz for the path F1-Pl2). Generally, the slopes of the curves given by the WBM seem to fit best with the measurements.

5. Conclusion

K_{ij} measurements were carried out on a half scaled test bench and analysed in a frequency range doubled in order to keep the same physical phenomena. The vibration transmission reductions through a double walls rigid junction (H) were examined and compared to other designs like Pi, λ, X and T-junctions. The conclusions in this paper concern only junctions whose ratio between the surface mass of the wall and that of the floor is approximately 0.28.

For all paths, an increase of the K_{ij} (± 1dB) is observed for each added wall. This is a small but relevant difference. As expected the non-interrupted path F1-F2 gives the lowest K_{ij} for all designs (between 0.9 and 4.6 dB) and the paths involving two light gypsum walls interrupted by the floor give the highest values (between 17.9 and 21.7 dB depending on the design). The K_{ij} for the transmission path Pl1-Pl2 of the Pi-junction can be approximated by the K_{ij} of the transmission path Pl1-Pl3 of the equivalent X-junction. For the H- and λ-junction, the K_{ij} for the transmission path Pl1-Pl3 is unexpectedly higher (+1.2 dB) than for the transmission path Pl2-Pl3. For each design concerned, the path F1-Pl1 gives more or less similar results to the path F1-Pl2 because the floor F1-F2 was considered as a single subsystem. The three numerical models (SEA, WBM, FEM) agree well with the measurements if an offset is incorporated in the models. To extend the conclusions to other surface mass ratios, the measurements will continue with heavier walls.

ACKNOWLEDGEMENTS

REFERENCES

1 Poblet-Puig J., Guigou-Carter C., Amplified catalogue of vibration reduction index formulas for junction based on numerical simulations, *Proceedings of Internoise*, Hamburg, Germany, 21-24 August, (2016).

2 Dijckmans A., Vibration transmission across junctions of double walls using the wave approach and statistical energy analysis, *Acta Acustica united with Acustica*, Vol. 102 (2016) 488-502.

3 Dijckmans A. Wave based modelling of vibration transmission across junctions composed of rectangular single and double walls, *Acta Acustica united with Acustica*, Vol. 102 (2016) 1011-1026.

4 Kling C., Miniaturising a wall test facility, *Journal of Building Acoustics*, Vol. 14, N°4, 2007, 243-266.

5 Wittstock V., Schmelzer M., Kling C., On the use of scaled models in building acoustics, *Proceedings of Euronoise*, Paris, France, 29 June-4 July(2008).

6 ISO 10848-1 (2006), Acoustics – Laboratory measurement of the flanking transmission of airborne and impact sound between adjoining rooms – Part 1: Frame document

7 ISO 10848-4 (2010), Acoustics – Laboratory measurement of the flanking transmission of airborne and impact sound between adjoining rooms – Part 4: Application to junctions with at least one heavy element

8 EN-12354-1 (2000), Building Acoustics - Estimation of acoustic performance of buildings from the performance of elements – Part 1: Airborne sound insulation between rooms

9 Hopkins C., Crispin C., Poblet-Puig J., Guigou-Carter C., Regression curves for vibration transmission across junctions of heavyweight walls and floors based on infinite element methods and wave theory, *Applied Acoustics* 113 (2016), 7-21.

10 Poblet-Puig J., Guigou-Carter C., Using spectral finite elements for parametric analysis of vibration reduction index of heavy junctions oriented to flanking transmissions and EN-12354 prediction method, *Applied Acoustics* 99 (2015), 8-23.

11 Crispin C., De Geetere L., Ingelaere B., Extensions of EN 12354 vibration reduction index expressions by means of FEM calculations, *Proceedings of Internoise*, Melbourne, Australia, 16-19 November(2014).

12 Hopkins C., Vibration transmission between coupled plates using finite element methods and statistical energy analysis. Part 1: Comparison of measured and predicted data for masonry walls with and without apertures. *Applied Acoustics* 64 (2003), 955-973.

13 Mees P., Vermeir G., Structure-Borne sound transmission at elastically connected plates, *Journal of sound and vibration* (1993) 166(1), 55-76.